ARTICLE

A generic approach based on long-lifetime fluorophores for the assessment of protein binding to polymer nanoparticles by fluorescence anisotropy

Received 00th January 20xx,
Accepted 00th January 20xx

DOI: 10.1039/x0xx00000x

Marwa A. Ahmed,[a,b] Dóra Hessz,[c,d] Benjámin Gyarmati[c], Mirkó Páncsics,[a] Róbert E. Gyurcsányi,[a,e,f] Miklós Kubinyi,[c] and Viola Horváth*[a,f]

Quantitation of protein-nanoparticle interactions is essential for the investigation of the protein corona around NPs *in-vivo* and when using synthetic polymer nanoparticles as affinity reagents for selective protein recognition *in-vitro*. Here, a method based on fluorescence anisotropy measurement is presented as a novel, separation-free tool for the assessment of protein-nanoparticle interactions. For this purpose, a long-lifetime luminescent Ru-complex is used for protein labelling, which exhibits low anisotropy when conjugated to the protein, but displays high anisotropy when the proteins are bound to the much larger polymer nanoparticles. As a proof of concept, the interaction of lysozyme with poly(N-isopropylacrylamide-co-N-*tert*-butylacrylamide-co-acrylic acid) nanoparticles is studied and fluorescence anisotropy measurements are used to establish the binding kinetics, binding isotherm and a competitive binding assay.

Introduction

Synthetic nanoparticles (NPs) have emerged as indispensable tools in the biomedical field with key applications in medical diagnostics, regenerative medicine, drug delivery vehicles and in bioassays as novel affinity materials and signal enhancers.[1] In all these applications NPs interact with biological systems, therefore the understanding of the bio-nano interface, is of utmost importance.

Nanoparticles *in vivo* penetrate to virtually all parts of the body including cells and organelles which leads to the immediate build-up of a protein layer on their surface. Since the seminal paper of Dawson[2], it is widely accepted that the biological impact of the NPs is fundamentally influenced by the nature and organization of the associated proteins, the protein corona.[3] The protein corona is composed of proteins with a wide range of affinity constants and on-off rates and its evolution is highly dynamic, involving kinetically driven and equilibrium binding processes. It is essential to gain quantitative information about these processes to understand how they influence the behaviour and functionality of NPs in biological systems. Protein binding is also important when using nanoparticles for *in vitro* bioassays in biological fluids. Besides the "conventional" use of NPs to enhance detection sensitivity, they can be also engineered to act as fully synthetic affinity ligands for the selective quantitation of proteins in biofluids. For example, poly(N-isopropylacrylamide) (PNIPAm) nanoparticles with functional co-monomers complementary to various amino acid residues, can be selected from small combinatorial libraries to bind a specific protein.[4] In addition, molecular imprinting of polymer NPs using solid phase bound template proteins results in high affinity and high selectivity nanoMIPs (molecularly imprinted nanoparticles).[5,6] Such NPs are expected to overcome the shortcomings of antibodies by providing better stability, cost-effectiveness, as well as the convenience of reproducible chemical synthesis. All these polymer NPs capture and concentrate the target protein from biological samples selectively, and the protein binding needs to be quantitated.

Currently the conventional approach to quantify the protein-NP interaction relies on the separation of the free and NP bound proteins by either centrifugation, magnetic force (in case of magnetic NPs) or size exclusion chromatography[7], followed by the analysis of the protein(s) with simple colorimetric assays, ICP-MS or LC-MS-MS[8]. However, low affinity interactions, which exhibit high dissociation rates, cannot be studied in this way, because the fast dissociation of the complex after separation perturbs the equilibrium. The separation-free methods are more powerful in this respect, but their use is generally limited either to particular types of nanoparticles, to high protein concentrations or involve immobilization of one of the reagent partners.[9] Thus, fluorescence quenching upon protein-NP binding, which uses the intrinsic fluorescence of proteins[10] and fluorescent labels[11] or fluorescent NPs[12], is mostly limited to

[a] *Department of Inorganic and Analytical Chemistry, Faculty of Chemical Technology and Biotechnology, Budapest University of Technology and Economics, Műegyetem rkp. 3., H-1111 Budapest, Hungary.*
[b] *Department of Chemistry, Faculty of Science, Arish University, 45511 El-Arish, North Sinai, Dahyet El Salam, Egypt*
[c] *Department of Physical Chemistry and Materials Science, Faculty of Chemical Technology and Biotechnology, Budapest University of Technology and Economics, Műegyetem rkp. 3., H-1111 Budapest, Hungary*
[d] *MTA-BME "Lendület" Quantum Chemistry Research Group, Műegyetem rkp. 3., H-1111 Budapest, Hungary*
[e] *MTA-BME "Lendület" Chemical Nanosensors Research Group, Műegyetem rkp. 3., H-1111 Budapest, Hungary*
[f] *ELKH-BME Computation Driven Chemistry Research Group, Műegyetem rkp. 3., H-1111 Budapest, Hungary*

† Electronic Supplementary Information (ESI) available: [details of any supplementary information available should be included here]. See DOI: 10.1039/x0xx00000x

inorganic NPs, where fluorescence quenching is much more pronounced. Isothermal titration calorimetry commonly applied to determine the affinity constant and enthalpy change of the binding needs a large amount of purified protein.[4,13] Fluorescence correlation spectroscopy (FCS), which follows the increase in the hydrodynamic radius of NPs upon protein adsorption[14,15], is limited to <100 nm NP size, moreover, requires fluorescent protein or NP probes. Surface plasmon resonance (SPR)[4,5,16] or quartz crystal microbalance (QCM)[4,17] measurements are label-free methods, but they rely on NP immobilization on planar surfaces or on NPs with plasmonic properties. FCS, SPR and QCM can provide information about the binding kinetics as well.

Hence, it would be of interest to develop a more generic separation-free method to sensitively quantify protein binding to nanoparticles. To not be limited by the particular properties of the nanoparticles, their generally larger size than that of the proteins could be exploited as a generic property. In this respect fluorescence polarization/anisotropy as a cheap and fast separation-free way to measure protein-ligand interactions in real-time (appropriate for kinetic analysis), even in a high-throughput manner, contours as a particularly suitable technique. Although the Lakowicz group demonstrated earlier that fluorescence polarization immunoassay (FPIA) for larger protein antigens is feasible with suitable selected fluorophores[18], this technique is largely limited to the assessment of low-molecular weight compounds.

Here we put forward a new approach to quantitate protein-nanoparticle interactions based on measuring fluorescence anisotropy by using long-fluorescence lifetime fluorophores (τ > several hundred ns) as protein labels. With conventional fluorophore labels of a few ns fluorescence lifetimes, this is not possible due to the inherently high anisotropy of the labelled proteins that would not change significantly upon binding to a NP. However, with long fluorescent lifetime fluorophores, the rotational correlation time of the labelled protein becomes insignificant on this timescale and low anisotropy is expected. Since NPs possess several orders of magnitude higher molecular weights than antibodies, the protein binding to the NPs would result in significantly higher rotational correlation times, i.e., significantly higher anisotropy values. Thus, we hypothesised that the protein-nanoparticle interaction could be sensitively detected and quantified in this way (Scheme 1).

To test this hypothesis, in the present work, the interaction of the antimicrobial enzyme, lysozyme with polymer nanoparticles is studied by steady-state anisotropy measurements. A long-lifetime, asymmetrical Ru-complex probe is used as the protein label, which displays high anisotropy in the frozen state.[18] Poly(N-isopropylacrylamide-co-N-*tert*-butylacrylamide-co-acrylic acid) nanoparticles (PNPs) with an optimized ratio of the co-monomers are utilized, as they have been shown earlier to possess high selectivity towards lysozyme.[19] Such type of polymers is at the core of nanoMIPs. Besides its direct application for the characterization of binding interactions, the bioanalytical use of the proposed approach is also shown through the quantitative assessment of lysozyme by competitive binding to the selective PNPs.

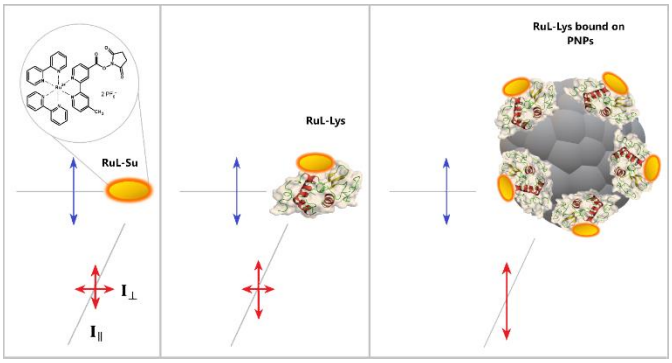

Scheme 1: Schematic representation of the proposed fluorescence anisotropy method. The long-lifetime fluorescent probe ((bis(2,2'-bipyridine)-4'-methyl-4-carboxy-pyridine-ruthenium N-succinimidyl ester-bis(hexafluorophosphate); RuL-Su) has close to zero anisotropy, i.e., it emits depolarized light (red arrows), when excited by a polarized light (blue arrows). The anisotropy of the emitted light increases only to a small value when the probe is bound to the protein (RuL-Lys), due to the long lifetime of the fluorophore. However, the anisotropy increases drastically, when the protein-probe conjugate binds to the polymer nanoparticle (PNP), thereby the protein-nanoparticle interaction can be detected.

Experimental

Materials and methods

Chemicals. All reagents used were at least of analytical grade. N-isopropylacrylamide (NIPAm), acrylic acid (AAc), N,N'-methylene bisacrylamide (BIS), ammonium persulfate (APS), sodium dodecyl sulfate (SDS), N,N-dimethylformamide (DMF), freeze-dried Micrococcus lysodeikticus, lysozyme from chicken egg white (MW 14.3 kDa, pI 11.35) and bis(2,2'-bipyridine)-4'-methyl-4-carboxypyridine-ruthenium N-succinimidyl ester bis (hexafluorophosphate) (RuL-Su) were obtained from Sigma-Aldrich (Burlington, MA, USA). N-tert-butylacrylamide (TBAm) was purchased from Tokyo Chemical Industry (Tokyo, Japan). NIPAm was recrystallized from hexane and AAc was passed through an aluminium oxide inhibitor remover column (Sigma-Aldrich) before use. Ultrapure water was produced by a Millipore Direct-Q system (Merck).

Synthesis of the polymer nanoparticles and conjugation of the Ru-complex to the protein. PNPs were synthesized by an aqueous precipitation polymerization method[20,21], copolymerizing N-isopropylacrylamide (53 mol%), N-tert-butylacrylamide (40 mol%), acrylic acid (5 mol%) and N,N'-methylene bisacrylamide (2 mol%) with a total monomer concentration of 130 mM. The specific protocol and the characterization of the of the PNPs can be found in the ESI.

The asymmetrical Ru-complex, (bis(2,2'-bipyridine)-4'-methyl-4-carboxy-pyridine-ruthenium N-succinimidyl ester-bis(hexafluorophosphate) (Scheme 1) was conjugated to lysozyme (MW 14.3 kDa, pI 11.35) through its reactive NHS-ester group by using standard protocol[22]. The detailed synthesis and the determination of the dye/protein ratio in the labelled protein (RuL-Lys) are described in the ESI.

Spectroscopic measurements. UV-Vis absorption measurements were done on a JASCO V-550 UV-Vis

spectrophotometer (JASCO International Co. Ltd.). Luminescence spectra, fluorescence anisotropy spectra and fluorescence decay curves were measured by an FS5 spectrofluorometer (Edinburgh Instruments) equipped with two αBBO type polarizers. In the steady state measurements, a 150 W xenon lamp was used at an excitation wavelength of 457 nm. The fluorescence emission anisotropy spectra were recorded placing a 550 nm long pass filter in the emission monochromator to eliminate the Rayleigh-scattered light. The anisotropy spectra were measured automatically in the range of 620-640 nm and the average anisotropies were taken. The temporal decay curves of the luminescence radiation were measured with time-correlated single photon counting (TCSPC) technique, using an EPL 450 pulsed diode laser (emission maximum at 441 nm, pulse width 90 ps) for excitation. All fluorescence spectroscopic experiments were carried out in a quartz microcuvette thermostated at 30 °C.

Measurement of protein-nanoparticle binding. Binding of the labelled protein or the Ru dye to different concentrations of PNPs without separation was assessed using steady-state anisotropy measurement. $1.6 \cdot 10^{-5}$ M RuL-Lys was incubated with $2.5 \cdot 10^{-3}$ up to 4 mg/mL PNP, while $8.9 \cdot 10^{-6}$ M RuL-Su was incubated with PNPs ($2.5 \cdot 10^{-3}$-1 mg/mL) in 10 mM phosphate buffer (pH 7.4) for 5 minutes at 30 °C in dark, and the steady-state anisotropy of the samples was measured.

Binding of lysozyme onto PNPs after separation was assessed by incubating $3.5 \cdot 10^{-7}$ M lysozyme with various concentrations of the PNPs (0.5-5 μg/mL) in phosphate buffer (10 mM, pH 7.4) for 20 minutes. A Vivaspin 500 (100kDa MWCO) centrifugal filter unit (Sartorius Stedim Lab Ltd., Stonehouse, UK) was utilized to separate the free and PNP-bound lysozyme by ultrafiltration. Centrifugation was carried out at 11,800 rcf for 20 minutes. The lysozyme activity of the filtrate was measured using the method of Shugar[23] (ESI) and its concentration was calculated from calibration with similarly filtered lysozyme standard solutions. Subtracting the unbound/total lysozyme concentration from 1, gave the ratio of the protein bound to the PNPs relative to the initial protein concentration (B/B_0).

To measure the adsorption isotherm, 0.1 mg/mL PNP was incubated with 0.31-51 μM concentrations of RuL-Lys in 10 mM phosphate buffer (pH 7.4) at 30°C and after 5 minutes the steady-state anisotropy was measured. From the anisotropy values the mole fraction of the nanoparticle bound protein (X) and the free protein (1-X) was calculated:

$$X = \frac{r - r_{RuL-Lys}}{r_{max} - r_{RuL-Lys}} \quad (1)$$

where r is the measured anisotropy at each concentration level, $r_{RuL\text{-}Lys}$ is the steady-state anisotropy of the labelled protein and r_{max} is the maximum anisotropy when all the labelled protein is bound to the PNPs. From this, the equilibrium concentrations can be obtained by equations 2 and 3:

$$c_e = c_0 \cdot (1 - X) \quad (2)$$

$$n_s = c_0 \cdot \frac{X}{m} \quad (3)$$

where c_e and c_0 are the equilibrium and initial molar concentrations of RuL-Lys, respectively, n_s is the equilibrium solid phase concentration of the bound protein in mol/g and m is the concentration of the PNPs (g/L).

In the competitive binding assay 16 μM RuL-Lys was mixed with different concentrations of lysozyme (0-2.92 mM) then 0.1 mg/mL PNP was added in 10mM phosphate buffer (pH 7.4) and the samples were incubated for 5 minutes at 30°C. Afterwards, the steady-state anisotropy was measured.

Results and discussion

Preparation and characterization of the poly (N-isopropylacrylamide) based nanogel and the Ru-complex labelled protein

PNPs were synthesized with high monomer conversion (93%) to obtain a stable colloidal suspension of 14.2 mg/mL concentration. The mean diameter and "molar concentration" of the nanogel preparation as determined by nanoparticle tracking analysis was 106 ± 2 nm and $1.78 \cdot 10^{-7}$ M ($1.07 \cdot 10^{14}$ particles/mL), respectively. Based on these, the average molecular weight of the PNPs was calculated to be ca. 80 MDa. Assuming spherical particles, their average volume and surface was estimated to be $1.08 \cdot 10^{6}$ nm^3 and $4.17 \cdot 10^{4}$ nm^2, respectively, taking into account their size distribution, as well.

To label lysozyme, we have used the asymmetrical Ru-complex, (bis(2,2'-bipyridine)-4'-methyl-4-carboxy-pyridine-ruthenium N-succinimidyl ester-bis(hexafluorophosphate); RuL-Su) that reacts directly with the exposed primary amines of the lysozyme. This Ru-complex has several advantages, as it has long luminescence lifetime, a large Stokes-shift, high limiting anisotropy (the anisotropy in rigid media) and is not very sensitive to oxygen quenching.[18]

The absorption spectra of the unconjugated ruthenium probe, RuL-Su and the probe-lysozyme conjugate, RuL-Lys show a strong absorption band at 280 nm and another characteristic peak at 457 nm (see Fig. S1†). Detailed interpretation of the spectra can be found in the ESI. The degree of labelling, i.e., the dye/protein ratio in the labelled protein (RuL-Lys) was determined by absorption spectroscopy to be 0.4, assuming that the molar absorptivity of the conjugated dye is the same as that of the free dye (19,200 M^{-1}cm-1 at 457 nm).

The emission spectra of RuL-Su, and that of RuL-Lys in the absence, and in the presence of PNPs are shown in Fig. 1. The emission wavelength maxima are collected in Table 1.

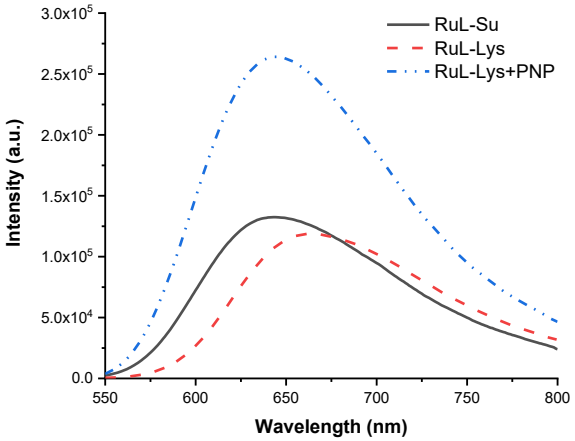

Fig. 1: Emission spectra of RuL-Lys (with and without PNPs) and RuL-Su at λ_{ex}=457 nm, recorded in 10mM phosphate buffer, pH 7.4.

Table 1. Luminescence spectral data of RuL-Su, and the RuL-Lys conjugate, both in the absence and in the presence of PNPs.

	λ_{em} (nm)	τ* (ns)	r_{st} (-)
RuL-Su	644	340 (100)	≈ 0
RuL-Lys	663	420 (100)	0.0045
RuL-Lys + PNPs	642	420 (13) 1100 (87)	0.12
RuL-Su + PNPs	644	340 (53) 898 (47)	not measurable**

where λ_{em}, τ and r_{st} are the wavelength corresponding to the emission maximum, the fluorescence lifetime and the steady-state anisotropy, respectively

* values in brackets are the relative amplitudes in eq. 4

**due to the weak interaction

The emission spectrum of RuL-Su involves a single band which is assigned to the transition from the ^{3}MLCT triplet state to the singlet ground state, S_0. The emission maximum of RuL-Su is shifted to longer wavelengths (from 644 nm to 663 nm) when the dye is conjugated to lysozyme and is shifted back, close to the original wavelength, when the conjugate is adsorbed on PNPs. The redshift of the emission band of the $Ru(bpy)_3$ fluorophore has also been observed for its conjugates with other proteins.[24,25] The blueshift of the emission accompanying the adsorption of the RuL-Lys conjugate is probably related to the restriction of the structural relaxation of the excited Ru label at the surface of PNPs.[26]

The free RuL-Su complex and the RuL-Lys conjugate have similar luminescence intensities, whereas the adsorption of the conjugate on PNPs induces a significant luminescence enhancement (Fig. 1). The main nonradiative deexcitation channels of Ru bipyridyl complexes, competing with the radiative process, are the internal conversion (IC) from the ^{3}MLCT to a dark ^{3}MC state and the ^{3}MLCT→S_0 intersystem crossing (ISC)[27]. The diminished conformational flexibility of the probe in the adsorbed protein decreases the probability of IC, therefore the quantum yield increases. In addition, the luminescence of the free RuL-Su complex and the RuL-Lys conjugate is also reduced by quenching due to water[28] and dissolved O_2[29]. The PNP restricts the access of oxygen to the adsorbed RuL-Lys molecules and photoluminescence increases because of the diminished quenching effect.

To obtain the fluorescence lifetime of the different species, luminescence decay curves of RuL-Su and RuL-Lys, both with and without PNPs were measured using a 441 nm pulsed laser for excitation and setting the detection wavelength to 660 nm. The decay curves were fitted by a single exponential function or by the sum of two exponentials:

$$I(t) = \sum_{i=1\ or\ 1,2} A_i exp(-t/\tau_i) \qquad (4)$$

where A_i is the pre-exponential factor, τ_i is the lifetime of the i-th component, and t is time. Fluorescence decay times of the different species are summarized in Table 1. The decay of RuL-Su and the RuL-Lys conjugate was found to be monoexponential. The conjugate incubated with PNPs produced a biexponential decay, with a major component belonging to the adsorbed and a minor component to the non-adsorbed conjugate. As expected, the lifetime of the PNP-bound labelled protein increases compared to the free protein-dye conjugate along with the luminescence intensity. The dye with PNPs also showed a biexponential decay indicating some adsorption.

Steady state anisotropy measurements were carried out on the different species using 457 nm excitation wavelength and a 550 nm long-pass filter, to eliminate scattered light from the NPs[30]. Anisotropy emission spectra were taken in the 620-640 nm range and an average anisotropy value was calculated. The measurement results are collected in Table 1. As expected, the ≈0 anisotropy of the free Ru-label barely increased upon conjugation to the protein, but a high anisotropy of r_{st}=0.12 was observed when the protein bound to the PNP.

Detection of protein binding on PNPs

To investigate the binding kinetics of RuL-Lys onto PNPs, the nanoparticles were mixed with the labelled lysozyme solution and the steady-state anisotropy was measured after different time intervals. The results are plotted in Fig. 2.

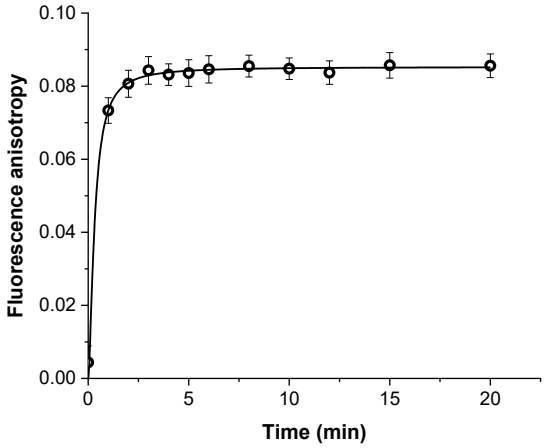

Fig. 2: Anisotropy change during incubation of RuL-Lys with PNPs. ($c_{RuL\text{-}Lys}$=5·10^{-5} M; c_{PNP}=0.1 mg/mL in 50 mM phosphate buffer, pH = 7.4, 30 °C).

We observed a rapid initial increase in the anisotropy, indicating a fast adsorption of RuL-Lys to the PNPs. Saturation is already achieved after 3 minutes. Though, in the present set up, with collection of full anisotropy emission spectra, only a data acquisition rate of ca. 1 data point per minute can be achieved, this experiment suggests that it is possible to follow protein-nanoparticle interactions in real-time (e.g., by filter-based instruments).

To assess the affinity of the labelled lysozyme to the PNPs, we have incubated RuL-Lys with increasing concentrations of nanoparticles and measured the steady-state anisotropy (Fig. 3).

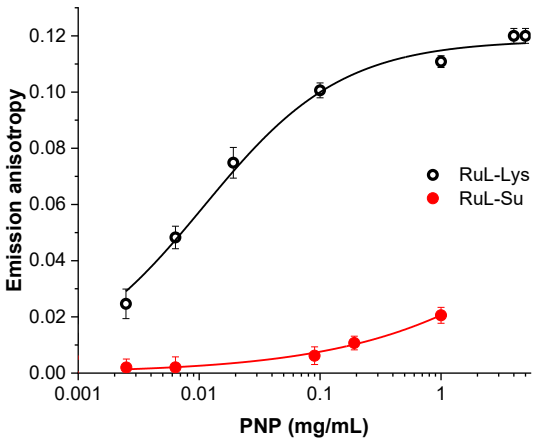

Fig. 3: Anisotropy of 1.6·10^{-5} M RuL-Lys (black open circles) or 8.9·10^{-6} M RuL-Su (red filled circles) incubated with different concentrations of PNPs (10 mM phosphate buffer, pH 7.4; 30°C)

As shown by Fig. 3, the emission anisotropy of RuL-Lys increases drastically with the PNP concentration in the lower PNP concentration range, as more and more labelled protein is bound by the polymer nanoparticles, the rotation of which is very slow. Finally, the anisotropy reaches a maximum value of r_{max}=0.12, where all the labelled protein is bound.

As a control, a similar experiment was performed to assess the binding of the unconjugated dye to different concentrations of PNPs, to confirm that the adsorption to the PNPs is due to the protein. The results presented in Fig. 3, show that ca. three decades larger PNP concentrations are needed to achieve similar anisotropy values as in the case of RuL-Lys, and even the highest applied PNP concentration is not enough to achieve r_{max}, i. e. to bind all the RuL-Su. This indicates that the Ru complex is bound to the PNPs with much lower affinity than the protein so that its contribution to the binding of the RuL-Lys conjugate is insignificant.

The adsorption isotherm of the labelled protein on the PNPs (Fig. 4). was determined by incubating 0.1 mg/mL PNP with increasing concentrations of RuL-Lys. The anisotropy values recorded after 5 minutes incubation were plotted as a function of the initial RuL-Lys concentration.

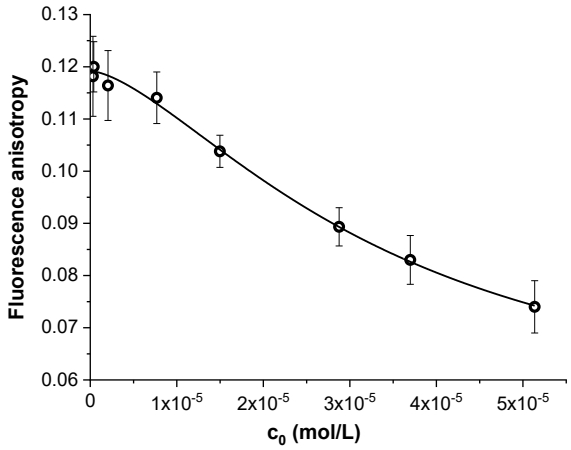

Fig. 4: Anisotropy of different concentrations of RuL-Lys incubated with 0.1 mg/mL PNP (10 mM phosphate buffer, pH 7.4; 30°C)

Below 2 µM concentration practically all RuL-Lys is bound to the PNPs, therefore the anisotropy is high, equal to r_{max}. When more lysozyme is added, the nanoparticles become saturated and the excess, free RuL-Lys decreases the anisotropy. From the anisotropy values, we could calculate at each concentration level c_e and n_s, the equilibrium solution and solid phase concentrations of the protein, respectively (eq. 1, 2 and 3). Hence the adsorption isotherm could be plotted as shown in Fig. 5.

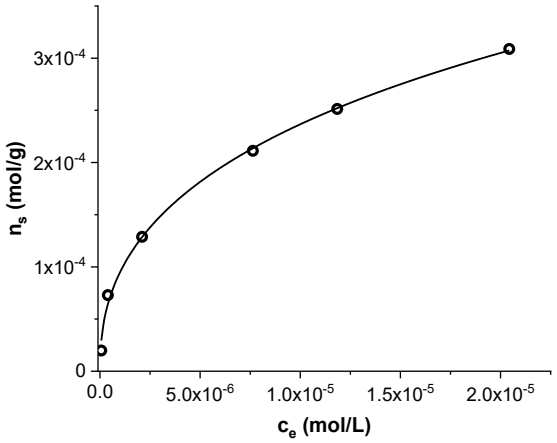

Fig. 5: Adsorption isotherm of RuL-Lys on PNPs. (0.1 mg/mL PNP was incubated with different concentrations of RuL-Lys in 10 mM phosphate buffer, pH 7.4 at 30°C)

Del Pino et al. have adapted the simple Hill model[31], originally used to depict the oxygenation of haemoglobin[32], to describe protein binding onto nanoparticles by reinterpreting the involved parameters.

The reinterpreted Hill-equation describing the interaction between proteins and NPs is:

$$\frac{N}{N_{max}} = \frac{(c_e)^n}{(K_D')^n + (c_e)^n} \quad (5)$$

and can be rewritten as

$$n_s = n_{max} \frac{(c_e)^n}{(K_D')^n + (c_e)^n} \quad (6)$$

where N - number of the adsorbed protein on the PNP surface, N_{max} – number of proteins on the nanoparticle surface at saturation, n_s - solid phase equilibrium concentration of bound protein, n_{max} - solid phase saturation concentration, c_e - equilibrium concentration of unbound protein in solution, K_D' - the equilibrium protein concentration producing half-saturation of the PNP surface and n - the Hill coefficient, an empirical parameter that reflects the cooperativity of binding.

We have fitted the above model on the isotherm points (R^2 of 0.9972) that enabled the calculation of K_D', $5.47 \cdot 10^{-4}$ M, which reflects the affinity of the PNP towards lysozyme. The maximum binding capacity of the PNPs (n_{max}) was $1.61 \cdot 10^{-3}$ mol/g. From this, and the weight and "molar" concentration of the nanoparticles (0.1 mg/mL and 1.25 pmol/mL, respectively), we could estimate the maximum number of proteins that can bind to a PNP. This way, N_{max} ≈ 130,000 was obtained. From the surface area of the PNP ($4.17 \cdot 10^4$ nm^2) and the smallest footprint of lysozyme (4.9 nm^2)[33], we estimated the maximum number of lysozyme on a PNP surface, assuming a closely packed monolayer coverage. This value is ≈8,500, therefore we might hypothesize that lysozyme is bound in many layers over the PNP, forming a protein corona. On the other hand, we can also speculate that lysozyme is not solely confined to the surface, but sequestered in the interior of the lightly crosslinked polymer network. An indirect support of the latter presumption is that such PNPs were found to protect lysozyme from thermal stress, which seems feasible if the PNP encapsulates the enzyme[34].

The value of the Hill coefficient, n, was 0.44, smaller than 1, indicating anti-cooperative binding, where protein adsorption suppresses further protein adsorption. This is a realistic scenario, since lysozyme, with a pI value of 11.35, is a highly positively charged protein at pH 7.4, therefore repulsive forces are hindering the incorporation of a next protein close to an already absorbed one.

To demonstrate the validity of the isotherm data obtained by anisotropy measurement, we have assessed the affinity of lysozyme to the PNPs with an independent, separation-based method. Unlabelled lysozyme was incubated with increasing concentrations of PNPs and, after equilibration, the free protein in the supernatant was separated from the NP bound protein by ultrafiltration. The free lysozyme was quantitated by measuring its enzymatic activity. The ratio of the bound (B) relative to the total protein concentration (B_0) was calculated and plotted as a function of the PNP concentration in Fig. 6. Using the isotherm parameters obtained from the adapted Hill fitting of the anisotropy data, we have also simulated this binding curve as shown in Fig. 6.

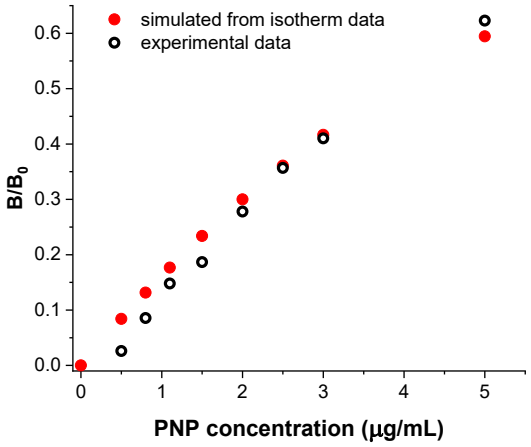

Fig. 6: Simulated and experimental binding curve of lysozyme to PNPs. ($3.5 \cdot 10^{-7}$ M lysozyme was incubated with different concentrations of PNPs in 10 mM phosphate buffer, pH 7.4)

We found a close agreement between the measured and calculated values. This indicates that the anisotropy measurement gives very similar results on the binding of lysozyme to the PNPs to those obtained by an independent method, which is based on the separation of the free and bound protein.

Competitive ligand binding assay

Finally, we demonstrated the applicability of the long-lifetime fluorophore-labelled protein in a competitive binding assay to

quantitate lysozyme concentration using the PNPs. In the competitive experiment, a mixture of a fixed amount of labelled lysozyme and increasing amount of unlabelled lysozyme competed for the binding sites of a fixed amount of PNP. Based on the affinity measurements, the amount of the labelled protein was chosen so that ≈80% of it was bound to PNPs initially. The steady-state emission anisotropies were measured after incubation. Values are plotted as a function of the unlabelled lysozyme concentration (Fig. 7a).

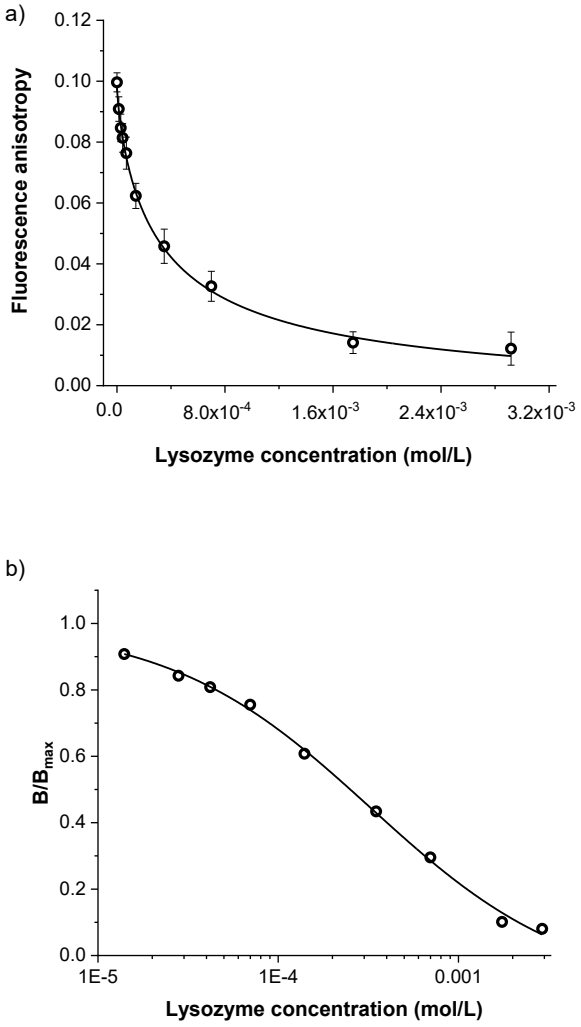

Fig. 7: a) Emission anisotropy in the competitive binding assay. ($c_{RuL\text{-}Lys}$=1.6·10^{-5} M; c_{PNP}=0.1 mg/mL at 30°C); b) Calibration curve for lysozyme fitted by a four-parameter logistic curve in the competitive binding assay.

As expected from competitive fluorescence polarization immunoassays, increasing the amount of the competing unlabelled analyte, less and less RuL-Lys can bind to the PNPs, therefore the fluorescence anisotropy decreases. At high concentration of unlabelled lysozyme, the anisotropy approached that of the free RuL-Lys. To obtain the calibration curve, the anisotropy values at different lysozyme concentrations (B) were normalized to the one obtained at zero concentration of the analyte (B_{max}), i. e. maximum binding of the labelled protein, and plotted against the analyte concentration in a logarithmic scale (Fig. 7b). The well-known sigmoid calibration curve was obtained, indicating that lysozyme was successfully competing for the PNP binding sites with the labelled lysozyme. A four-parameter logistic curve was fitted onto the data points. The IC50 value, i.e., the analyte concentration, that produces 50% inhibition of the binding of RuL-Lys, was evaluated from the curve as being 3.3·10^{-4} M.

Conclusions

Here, we introduce a fluorescence anisotropy measurement for the assessment of protein binding to nanoparticles. The approach is based on the use of a long-lifetime fluorophore to label the protein molecule. A consequence of the long fluorescence decay time of the label is that it's close to zero anisotropy does not increase substantially upon conjugation to the biomacromolecule. Only when the labelled protein binds to the nanoparticle that causes a very large size increase, increases the anisotropy value significantly, i.e., the dynamic range of the fluorescence anisotropy is shifted to much higher molecular weights of ≈10 MDa.

We demonstrated the new concept by studying the interaction of lysozyme, labelled with an asymmetrical Ru-complex and a multifunctional poly(NIPAm) nanoparticle, that can bind the lysozyme protein selectively. After determining the fundamental fluorescence spectral properties of the involved compounds, fluorescence anisotropy measurements were performed to study the binding kinetics and affinity of the labelled protein to the PNPs. The binding isotherm was also determined and an adapted Hill model fitted on the experimental data revealed the maximum number of binding sites for the protein on the PNP, the equilibrium dissociation constant and the cooperativity of the protein-PNP binding.

The results of the anisotropy measurements were validated with an independent separation-based method. The experimental equilibrium binding curve showed good correlation with the curve that was simulated using the isotherm parameters stemming from the anisotropy measurement. This demonstrates that the anisotropy measurement gives valid quantitative information on the protein-NP binding. Finally, a competitive binding assay format was set-up, and a calibration curve was established, which demonstrates the applicability of the fluorescence anisotropy measurement in quantitative protein assays using synthetic PNP affinity ligands.

The advantages of the proposed fluorescence polarization method are that it is sensitive, requires simple instrumentation, low sample amounts and most importantly, does not require the separation of the nanoparticle-bound and free-protein, nor immobilization of any of the interacting parts (protein or nanoparticle). This makes the technique very fast, enabling high-throughput screening of protein-nanoparticle interactions, even if the interaction is not very strong. A further notable benefit is that protein-NP binding kinetics can be measured real-time.

Author Contributions

R. E. Gy., V. H.: conceptualization; D. H.: formal analysis, visualization; R. E. Gy., B. Gy.: funding acquisition; M. A. A., D. H., M. P.: investigation; M. K.: methodology; V. H.: supervision, project administration; V. H., M. K., R. E. Gy.: writing original draft; B. Gy., writing – review & editing.

Conflicts of interest

There are no conflicts to declare.

Acknowledgements

The research reported in this paper is part of project no. BME-EGA-02, implemented with the support provided by the Ministry of Culture and Innovation of Hungary from the National Research, Development and Innovation Fund, financed under the TKP2021 funding scheme. Further support was provided by the National Research, Development and Innovation (NRDI) Office, Hungary via grant FK 138029. B. Gy. and M. A. A. acknowledge the János Bolyai Research Scholarship of the Hungarian Academy of Sciences and the Stipendium Hungaricum Scholarship, respectively.
The authors greatly acknowledge the help of Dr. Adrien Paudics with the spectroscopic measurements and that of Norbert Kovács with the Nanosight measurements.

References

1 G. R. Rudramurthy and M. K. Swamy, *Journal of Biological Inorganic Chemistry*, 2018, **23**, 1185–1204.
2 I. Lynch and K. A. Dawson, *Nano Today*, 2008, **3**, 40–47.
3 P. C. Ke, S. Lin, W. J. Parak, T. P. Davis and F. Caruso, *ACS Nano*, 2017, **11**, 11773–11776.
4 J. O'Brien and K. J. Shea, *Acc Chem Res*, 2016, **49**, 1200–1210.
5 A. Poma, A. Guerreiro, S. Caygill, E. Moczko and S. Piletsky, *RSC Adv*, 2014, **4**, 4203–4206.
6 J. Xu, S. Ambrosini, E. Tamahkar, C. Rossi, K. Haupt and B. Tse Sum Bui, *Biomacromolecules*, 2016, **17**, 345–353.
7 R. García-Álvarez and M. Vallet-Regí, *Nanomaterials*, DOI:10.3390/nano11040888.
8 C. Carrillo-Carrion, M. Carril and W. J. Parak, *Curr Opin Biotechnol*, 2017, **46**, 106–113.
9 L. Li, Q. Mu, B. Zhang and B. Yan, *Analyst*, 2010, **135**, 1519–1530.
10 X. C. Shen, X. Y. Liou, L. P. Ye, H. Liang and Z. Y. Wang, *J Colloid Interface Sci*, 2007, **311**, 400–406.
11 M. Karlsson and U. Carlsson, *Biophys J*, 2005, **88**, 3536–3544.
12 L. Shang, S. Brandholt, F. Stockmar, V. Trouillet, M. Bruns and G. U. Nienhaus, *Small*, 2012, **8**, 661–665.
13 T. Cedervall, I. Lynch, S. Lindman, T. Berggård, E. Thulin, H. Nilsson, K. A. Dawson and S. Linse, *Proc Natl Acad Sci U S A*, 2007, **104**, 2050–2055.
14 L. Shang and G. U. Nienhaus, *Acc Chem Res*, 2017, **50**, 387–395.
15 S. Milani, F. Baldelli Bombelli, A. S. Pitek, K. A. Dawson and J. Rädler, *ACS Nano*, 2012, **6**, 2532–2541.
16 A. Patra, T. Ding, G. Engudar, Y. Wang, M. M. Dykas, B. Liedberg, J. C. Y. Kah, T. Venkatesan and C. L. Drum, *Small*, 2016, **12**, 1174–1182.
17 S. H. Brewer, W. R. Glomm, M. C. Johnson, M. K. Knag and S. Franzen, *Langmuir*, 2005, **21**, 9303–9307.
18 H. Szmacinski, E. Terpetschnig and J. R. Lakowicz, *Biophysical Chemistry* , 1996, **62**, 109–120.
19 K. Yoshimatsu, B. K. Lesel, Y. Yonamine, J. M. Beierle, Y. Hoshino and K. J. Shea, *Angewandte Chemie - International Edition*, 2012, **51**, 2405–2408.
20 J. D. Debord and L. A. Lyon, *Langmuir*, 2003, **19**, 7662–7664.
21 M. A. Ahmed, J. Erdőssy and V. Horváth, *Periodica Polytechnica Chemical Engineering*, 2020, **65**, 28–41.
22 G. Hermanson, Ed., *Bioconjugate Techniques*, Academic Press, 3rd edn., 2013.
23 D. Shugar, *Biochim Biophys Acta*, 1952, **8**, 302–309.
24 E. Terpetschnig, H. Szmacinski and J. Lakowicz, *Anal Biochem*, 1995, **227**, 140–147.
25 E. M. Ryan, J. G. Vos, R. O'kennedy, M. M. Feeney and J. M. Kelly, *Bioconjug Chem*, 1992, **3**, 285–290.
26 P. Innocenzi, H. Kozuka and T. Yoko, *Journal of Physical Chemistry B*, 1997, **101**, 2285–2291.
27 S. A. McFarland, D. Magde and N. S. Finney, *Inorg Chem*, 2005, **44**, 4066–4076.
28 J. Maillard, K. Klehs, C. Rumble, E. Vauthey, M. Heilemann and A. Fürstenberg, *Chem Sci*, 2021, **12**, 1352–1362.
29 K. Kalyanasundaram, *Coord Chem Rev*, 1982, **46**, 159–244.
30 C. E. Hunt and R. J. Ansell, *Analyst*, 2006, **131**, 678–683.
31 P. Del Pino, B. Pelaz, Q. Zhang, P. Maffre, G. U. Nienhaus and W. J. Parak, *Mater Horiz*, 2014, **1**, 301–313.
32 A. Hill, *Proceedings of the Physiological Society*, 1910, **40**, iv–vii.
33 R. M. Greer, B. A. Scruggs, R. A. May and B. D. Chandler, *Langmuir*, 2009, **25**, 7161–7168.
34 J. M. Beierle, K. Yoshimatsu, B. Chou, M. A. A. Mathews, B. K. Lesel and K. J. Shea, *Angewandte Chemie - International Edition*, 2014, **53**, 9275–9279.

35

